NMDA receptor hypofunction in Meg-01 cells reveals a role for intracellular calcium homeostasis in balancing megakaryocytic-erythroid differentiation

James I. Hearn, Taryn N. Green, Martin Chopra, Yohanes NS Nursalim, Leandro Ladvanszky, Nicholas Knowlton, Cherie Blenkiron, Raewyn C. Poulsen, Dean C. Singleton, Stefan K. Bohlander, Maggie L. Kalev-Zylinska

Supplementary data

Supplementary Fig. S1

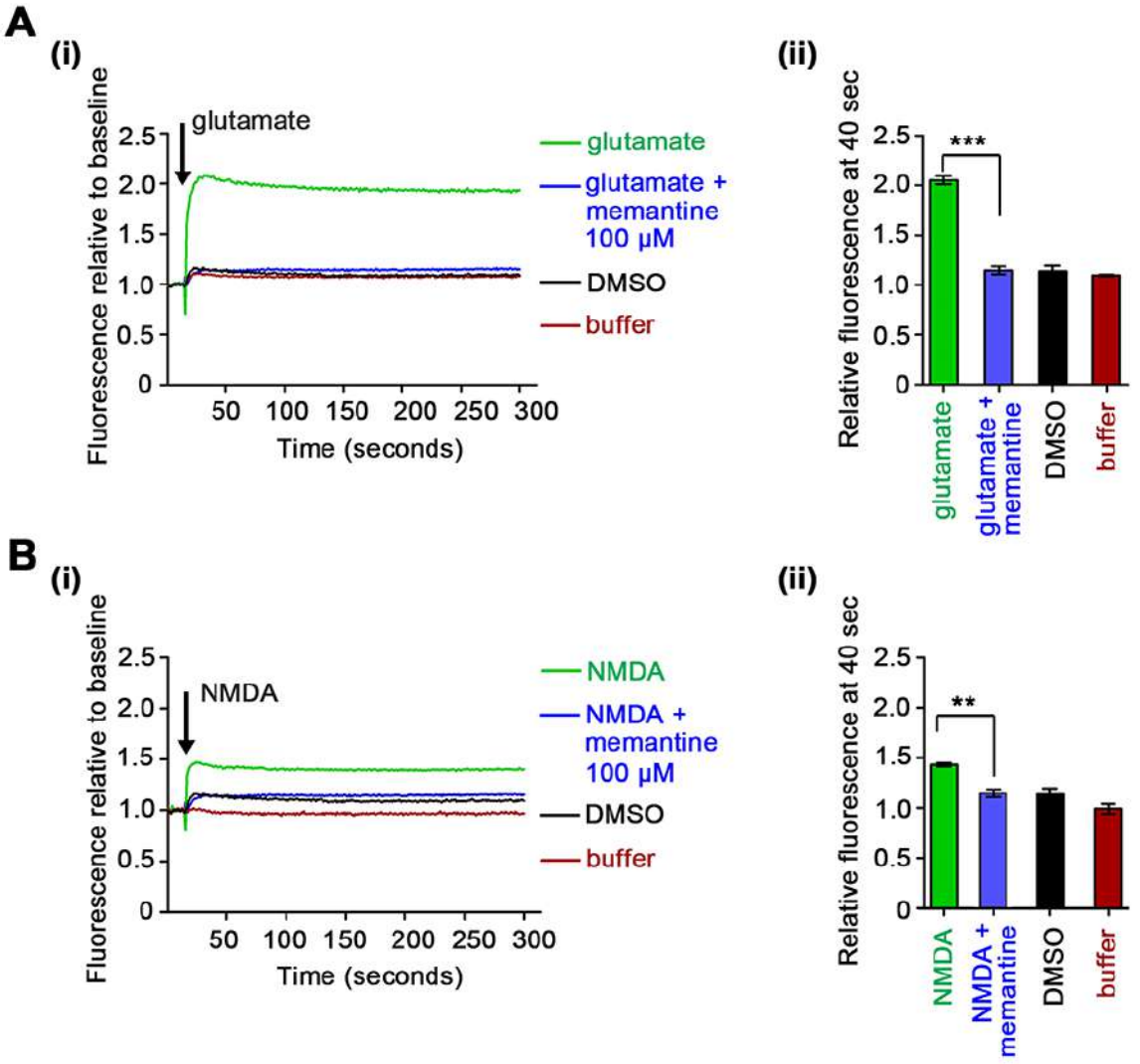

Supplementary Fig. S1. Modulation of NMDAR-evoked Ca^{2+} influx in Meg-01 cells using memantine. Unmodified Meg-01 cells were loaded with Fluo-4-AM and intracellular Ca^{2+} responses were recorded on a plate reader after the addition of glutamate 400 µM (**A**) and NMDA 50 µM (**B**) without and with memantine 100 µM, as described before [1]. Baseline fluorescence was recorded for 10 seconds, after which the activator was added, and measurements continued until 300 seconds. Memantine was aliquoted into wells just before

adding the activator. DMSO was used as a diluent, therefore it was added to buffer as an additional control. Line graphs in **A(i)** and **B(i)** show mean levels of Fluo-4-AM fluorescence over 300 seconds calculated from three independent experiments for each condition. Fold change was determined from the average fluorescence values acquired at baseline, set at 1.0. The bar graphs in **A(ii)** and **B(ii)** show mean ± SEM of relative fluorescence recorded for each condition at 40 seconds, when Ca^{2+} responses were near maximal. Each experiment was repeated at least three times using cells of different passages. Within each experiment, measurements were taken from triplicate wells. Statistical significance is shown (one-way ANOVA with Dunnett post-hoc; $^{**}P < 0.01$, $^{***}P < 0.001$).

Reference:

1 T Kamal, TN Green, JI Hearn et al. N-methyl-d-aspartate receptor mediated calcium influx supports in vitro differentiation of normal mouse megakaryocytes but proliferation of leukemic cell lines. Res Pract Thromb Haemost 2018;2:125-138.

Supplementary Fig. S2

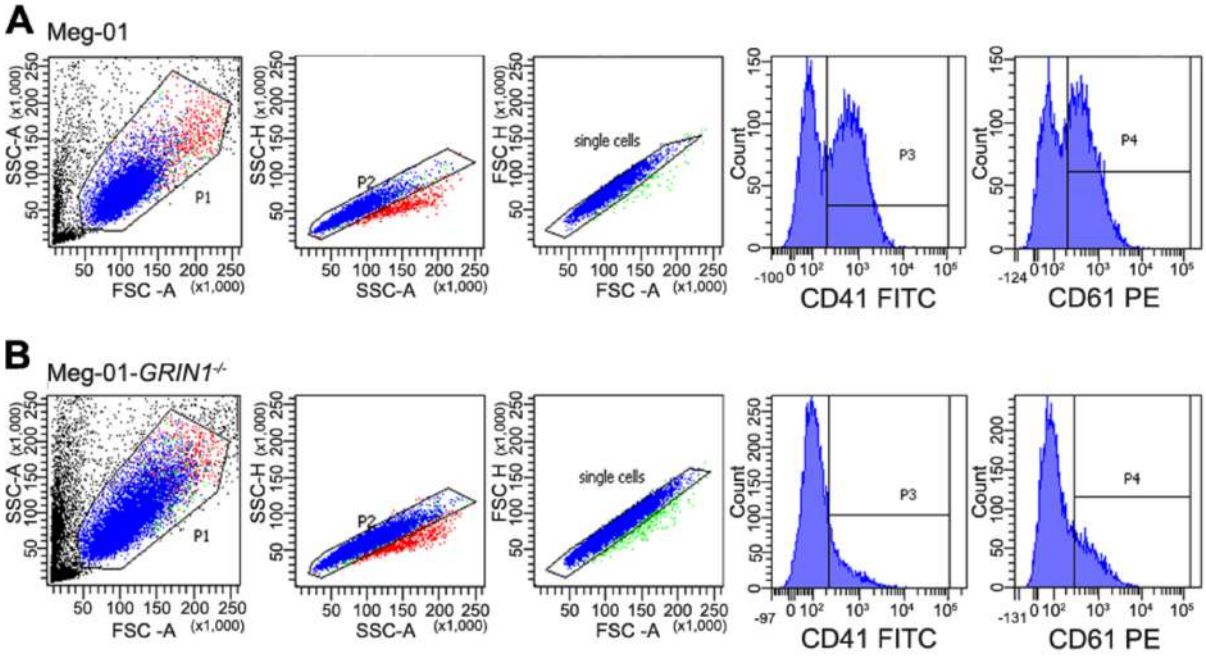

Supplementary Fig. S2. Flow cytometry gating for CD41 and CD61 on Meg-01 (**A**) and Meg-01-*GRIN1*$^{-/-}$ cells (**B**). Cells were gated based on forward and side scatter properties (FSC-A vs SSC-A). Cell doublets were excluded by gating on height and area for side scatter (SSC-H vs SSC-A) and forward scatter (FSC-H vs FSC-A), respectively. Histogram examples of CD41 and CD61 expression (CD41-FITC, CD61-PE) are shown.

Supplementary Fig. S3

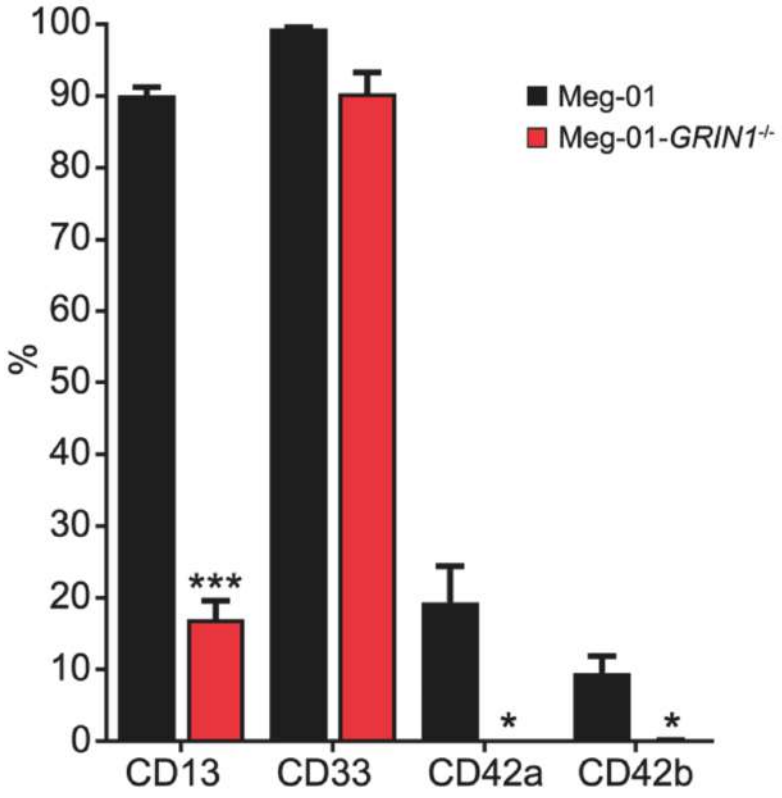

Supplementary Fig. S3. Expression of additional myeloid antigens on Meg-01 and Meg-01-*GRIN1*$^{-/-}$ cells. Bar graph showing expression of CD13, CD33, CD42a and CD42b on the surface of cells, examined by flow cytometry. Bars are mean ± SEM from at least three independent experiments. Statistical significance is shown where reached (unpaired Student t-test, 2-tailed; *$P < 0.05$, ***$P < 0.001$).

Supplementary Fig. S4

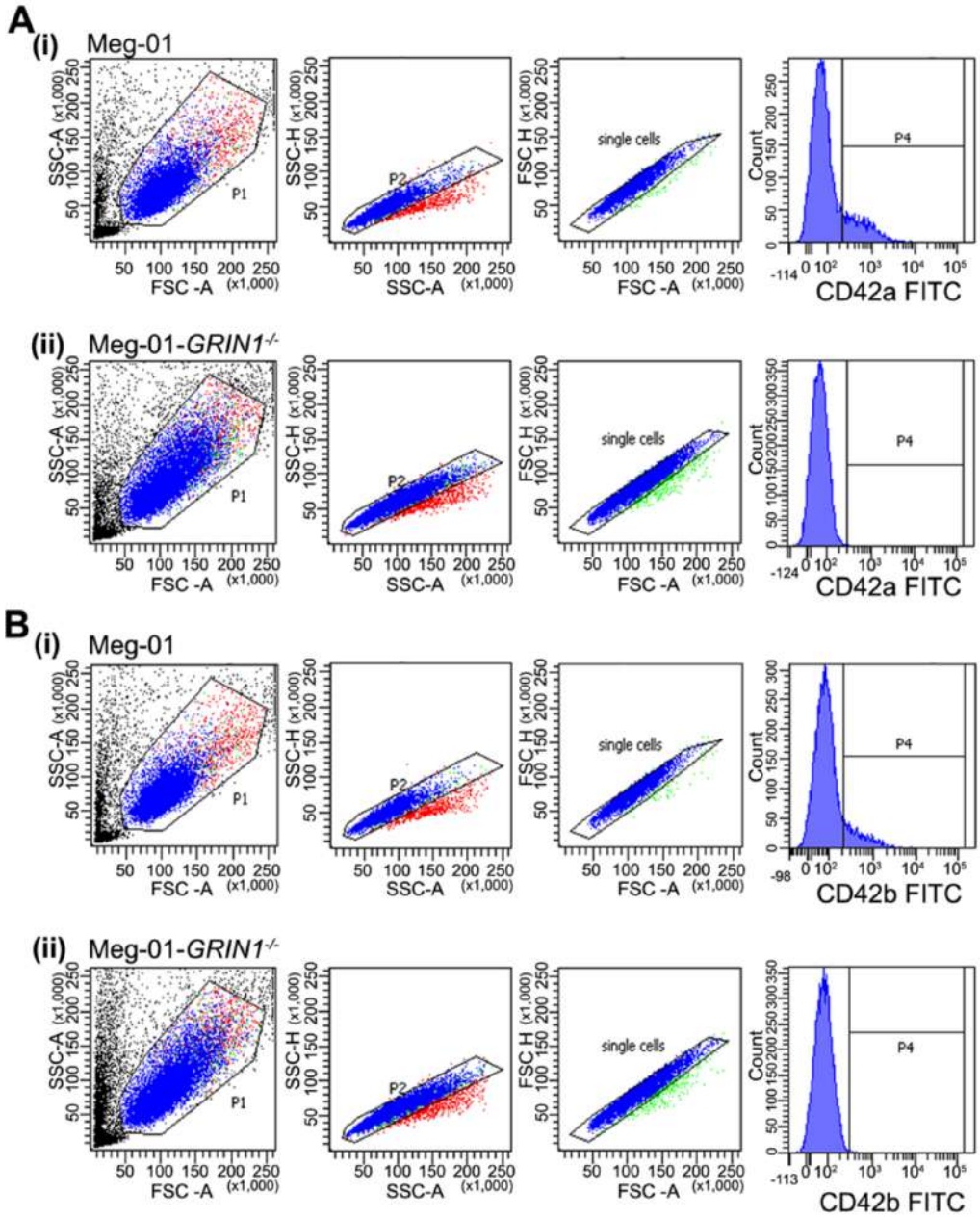

Supplementary Fig. S4. Flow cytometry gating for CD42a (**A**) and CD42b (**C**) on Meg-01 and Meg-01-*GRIN1*$^{-/-}$ cells (**i** and **ii**, respectively). Cells were gated based on forward and side scatter properties (FSC-A vs SSC-A). Cell doublets were excluded by gating on height and area for side scatter (SSC-H vs SSC-A) and forward scatter (FSC-H vs FSC-A), respectively. Histogram examples of CD42a and CD42b expression (CD42a-PE, CD42b-PE) are shown.

Supplementary Fig. S5

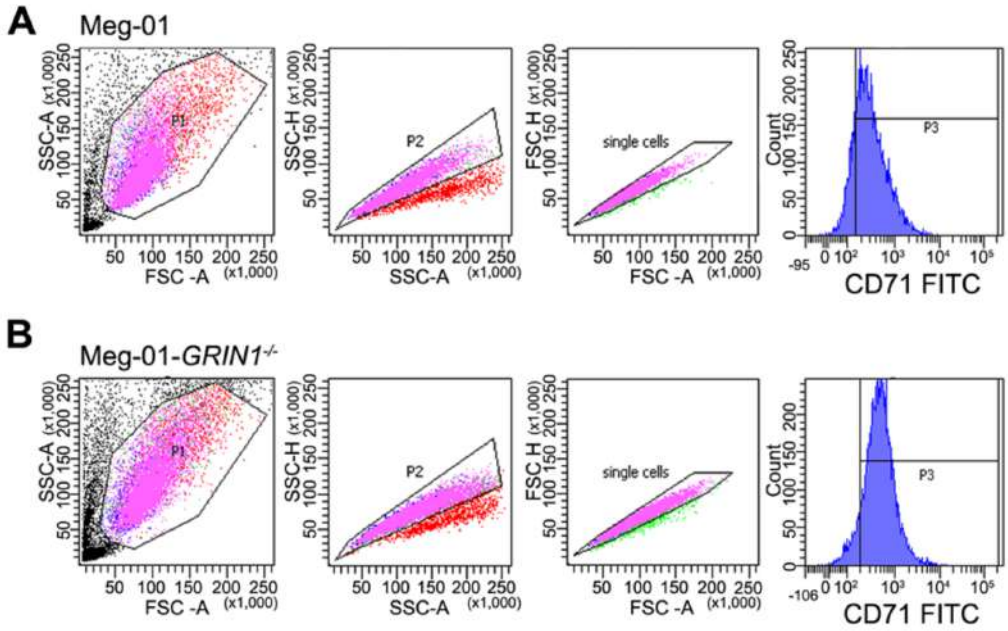

Supplementary Fig. S5. Flow cytometry gating for CD71 on Meg-01 (**A**) and Meg-01-*GRIN1*$^{-/-}$ cells (**B**). Cells were gated based on forward and side scatter properties (FSC-A vs SSC-A). Cell doublets were excluded by gating on height and area for side scatter (SSC-H vs SSC-A) and forward scatter (FSC-H vs FSC-A), respectively. Histogram examples of CD71 expression (CD71-FITC) are shown.

Supplementary Fig. S6

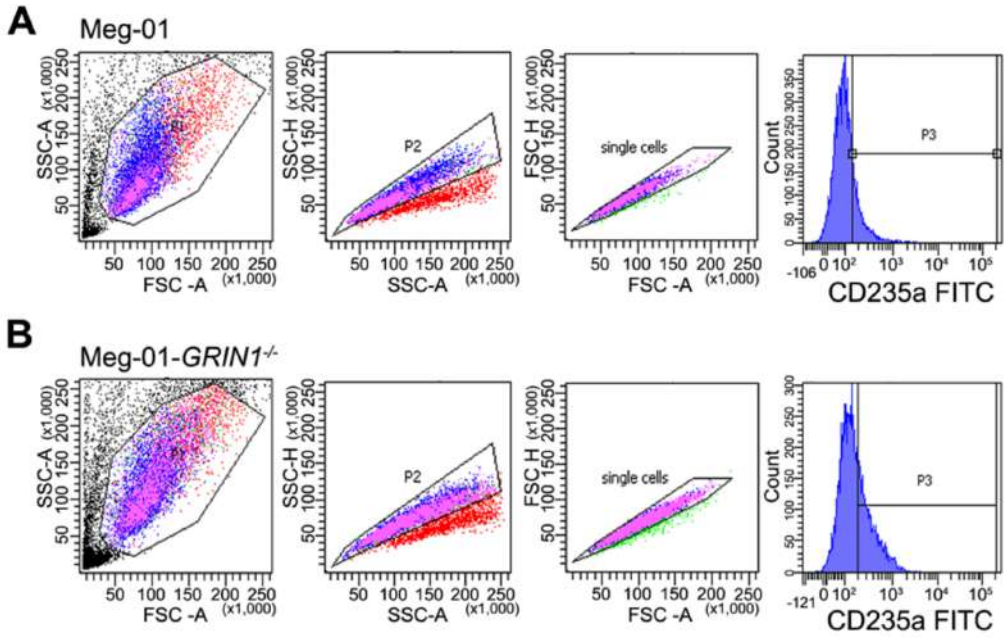

Supplementary Fig. S6. Flow cytometry gating for CD235a on Meg-01 (**A**) and Meg-01-*GRIN1*$^{-/-}$ cells (**B**). Cells were gated based on forward and side scatter properties (FSC-A vs SSC-A). Cell doublets were excluded by gating on height and area for side scatter (SSC-H vs SSC-A) and forward scatter (FSC-H vs FSC-A), respectively. Histogram examples of CD235a expression (CD235a-FITC) are shown.

Supplementary Fig. S7

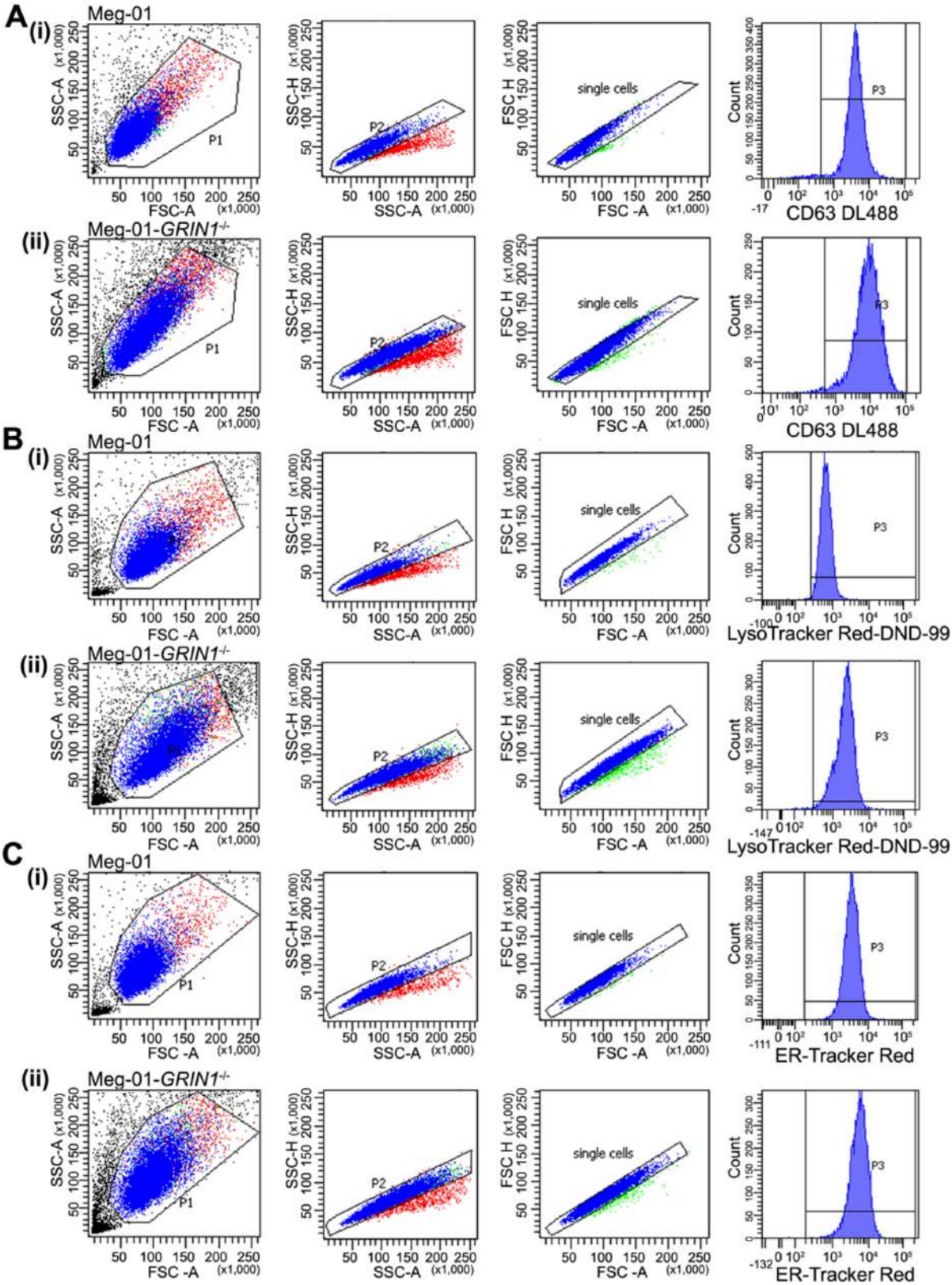

Supplementary Fig. S7. Flow cytometry gating for CD63 (**A**)**,** LysoTracker Red DND-99 (**B**) and ER-Tracker Red (**C**) on Meg-01 and Meg-01-*GRIN1*$^{-/-}$ cells (**i** and **ii**, respectively). Cells were gated based on forward and side scatter properties (FSC-A vs SSC-A). Cell doublets were excluded by gating on height and area for side scatter (SSC-H vs SSC-A) and forward scatter (FSC-H vs FSC-A), respectively. Histogram examples of CD63 (DL488), LysoTracker Red DND-99 and ER-Tracker Red are shown.

Supplementary Fig. S8

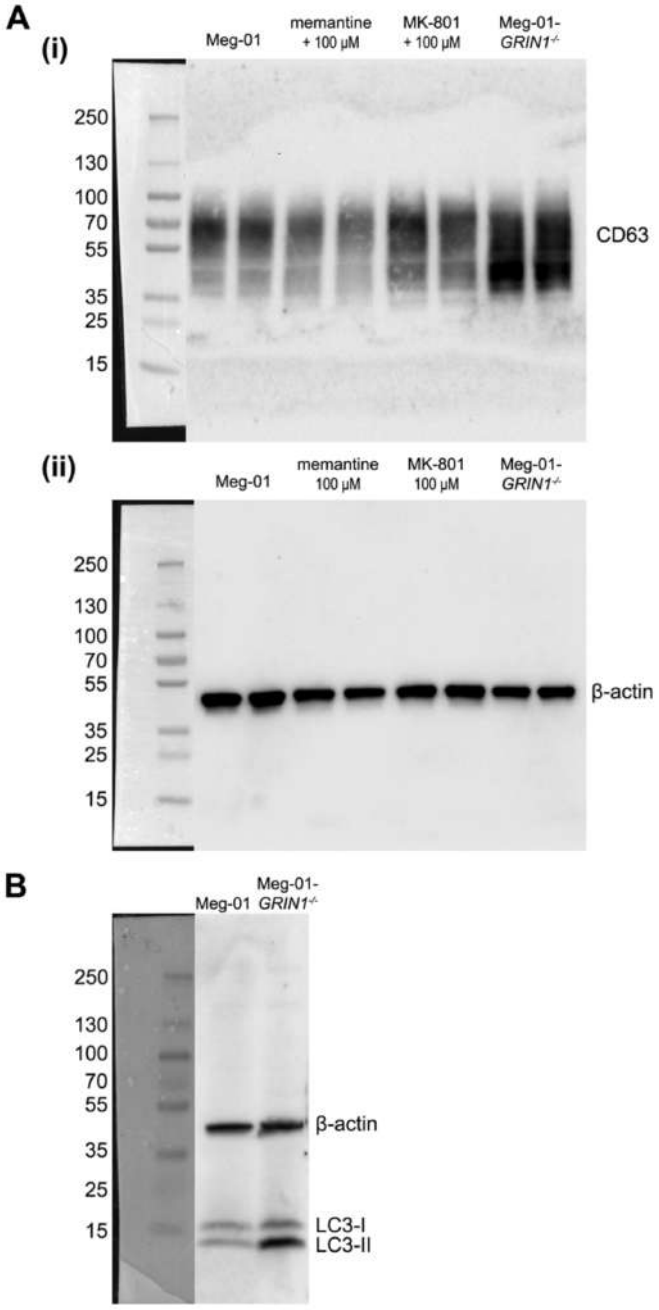

Supplementary Fig. S8. Western blots showing expression of CD63 and LC3 in Meg-01 and Meg-01-*GRIN1*$^{-/-}$ cells. These full size blots supplement data shown in **Fig. 4D**. (**A**) CD63 is shown in **Ai** with β-actin for the same blot in **Aii**. Other lanes contained lysates of Meg-01 cells cultured in the presence of memantine and MK-801 (both at 100 µM) as controls. (**B**) Lipidation of LC3 in Meg-01 and Meg-01-*GRIN1*$^{-/-}$ cells, including β-actin bands.

Supplementary Fig. S9

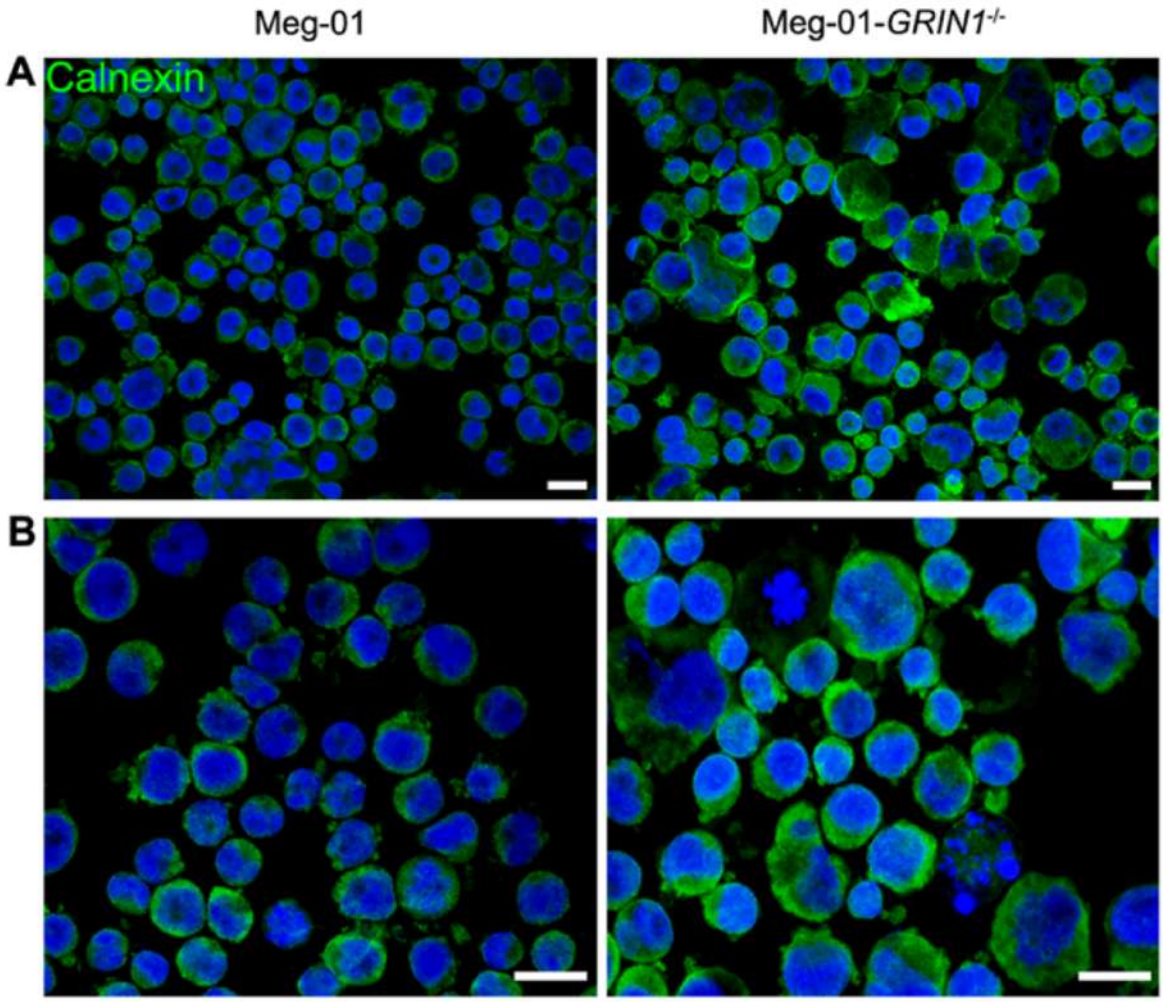

Supplementary Fig. S9. Calnexin immunofluorescence in Meg-01 and Meg-01-*GRIN1*$^{-/-}$ cells. Representative images are shown from three independent experiments at lower (20x, **A**) and higher (40x, **B**) magnifications that captured different fields of view. Staining is stronger in Meg-01-*GRIN1*$^{-/-}$ cells. Scale bars, 50 µm.

Supplementary Fig. S10

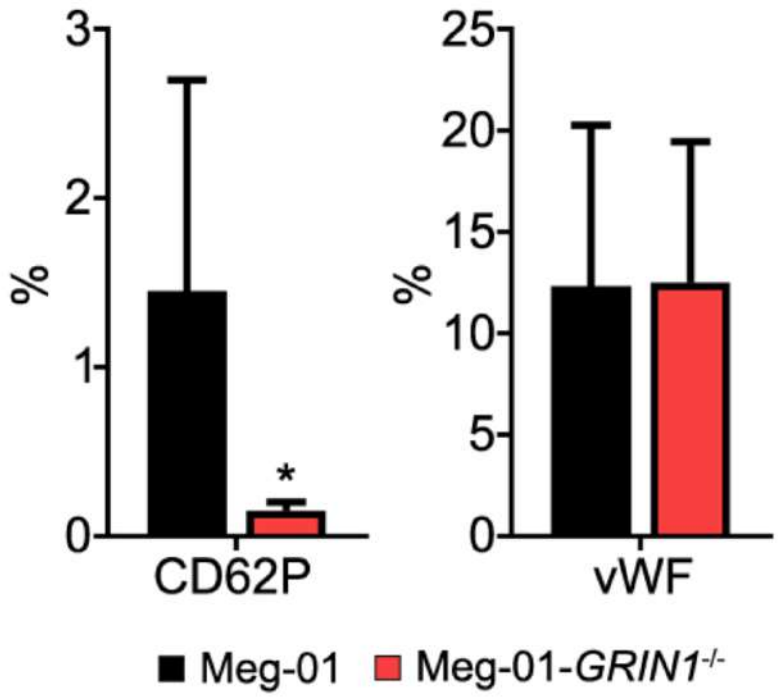

Supplementary Fig. S10. Expression of α-granule markers in Meg-01 and Meg-01-*GRIN1*$^{-/-}$ cells. Bar graph showing expression of CD62P and von Willebrand factor (vWF) inside cells, as examined by flow cytometry. Bars are mean ± SEM from at least three independent experiments. Statistical significance is shown where reached (unpaired Student t-test, 2-tailed; *$P < 0.05$).

Supplementary Fig. S11

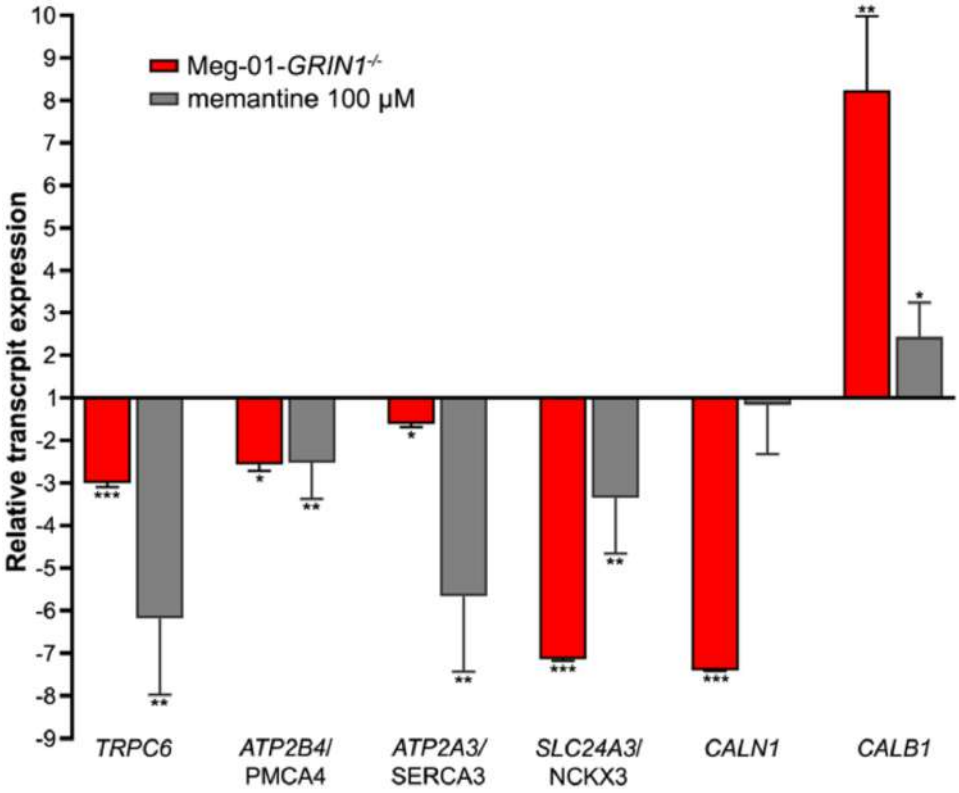

Supplementary Fig. S11. Memantine effects on selected calcium signalling molecules in Meg-01 cells. Bar graph showing relative transcript levels examined by RT-qPCR in Meg-01 cells cultured in the presence of memantine (100 µM) and in Meg-01-*GRIN1*$^{-/-}$ cells, graphed and analysed relative to unmodified Meg-01 cells. Bars are mean ± SEM from three independent experiments performed in triplicate. Statistical significance is shown where reached (one-way ANOVA with Dunnett post-hoc; *$P < 0.05$, **$P < 0.01$, ***$P < 0.001$). Abbreviations: RT-qPCR, quantitative reverse transcriptase-polymerase chain reaction.

Supplementary Fig. S12

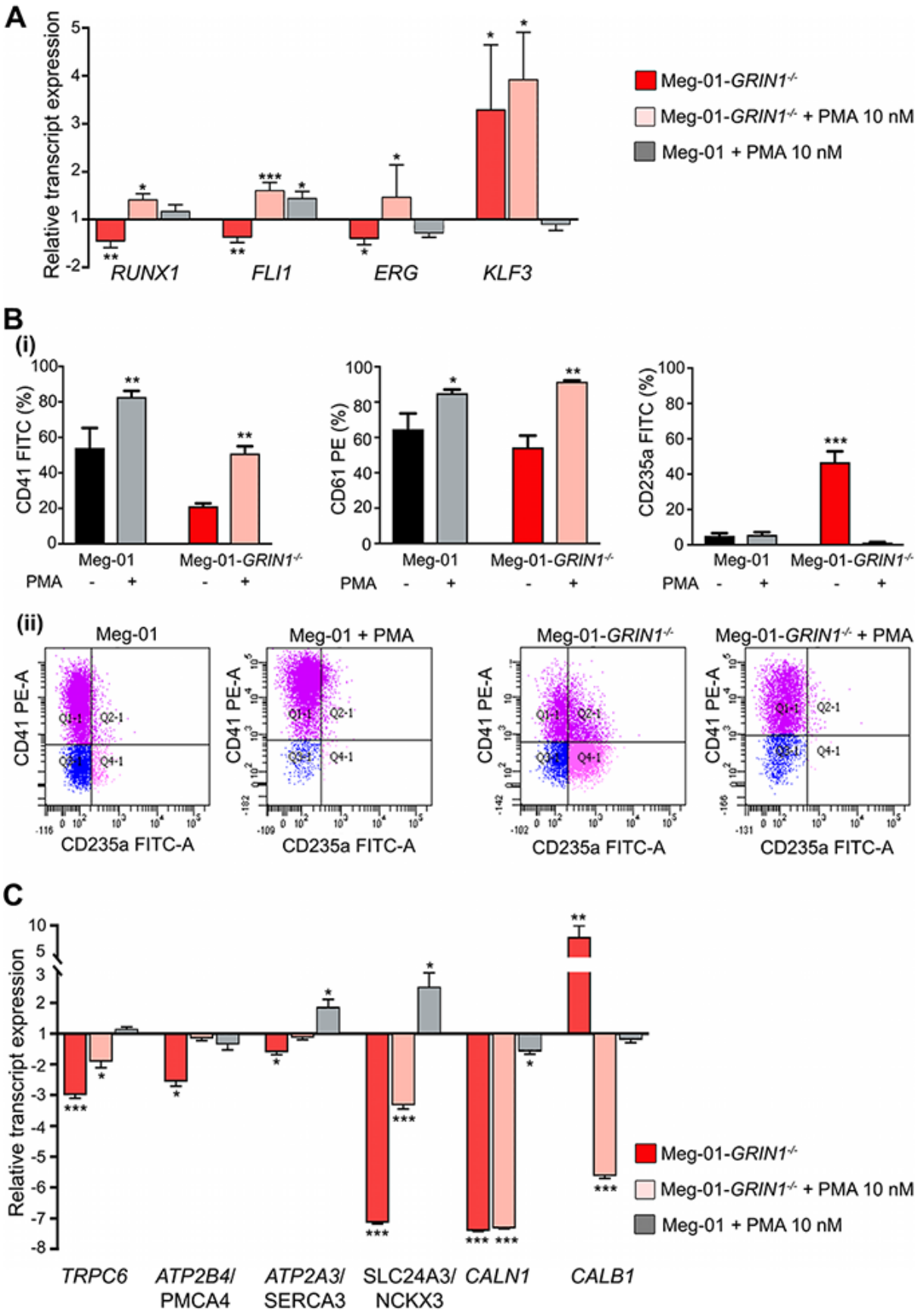

Supplementary Fig. S12. PMA effects on the phenotype of Meg-01 and Meg-01-*GRIN1*$^{-/-}$ cells. (**A**) Bar graphs showing relative transcript levels (compared with unmodified Meg-01 cells set at 1) of selected megakaryocytic-erythroid transcription factors examined by RT-qPCR in Meg-01 and Meg-01-*GRIN1*$^{-/-}$ cells before and after 3-day cultures with 10 nM PMA. (**B**) Expression of megakaryocytic and erythroid differentiation markers (CD41, CD61 and CD235a) examined by flow cytometry on Meg-01 and Meg-01-*GRIN1*$^{-/-}$ cells before and after PMA treatment. Bar graphs in **Bi** show mean ± SEM for percentage of cells expressing the CD markers. Dotplots in **Bii** show representative examples of CD41 and CD235a dual staining. Gating is shown in **Supplementary Fig. S14**. (C) Bar graphs showing relative transcript levels (compared with unmodified Meg-01 cells set at 1) of selected intracellular calcium regulators examined by RT-qPCR in Meg-01 and Meg-01-*GRIN1*$^{-/-}$ cells before and after PMA treatment. All bar graphs show mean ± SEM from three independent experiments (RT-qPCR data in triplicate). Statistical significance is shown where reached compared with unmodified Meg-01 cells as controls (one-way ANOVA with Dunnett post-hoc; $*P < 0.05$, $**P < 0.01$, $***P < 0.001$). Abbreviations: PMA, phorbol 12-myristate 13-acetate; RT-qPCR, quantitative reverse transcriptase-polymerase chain reaction.

Supplementary Fig. S13

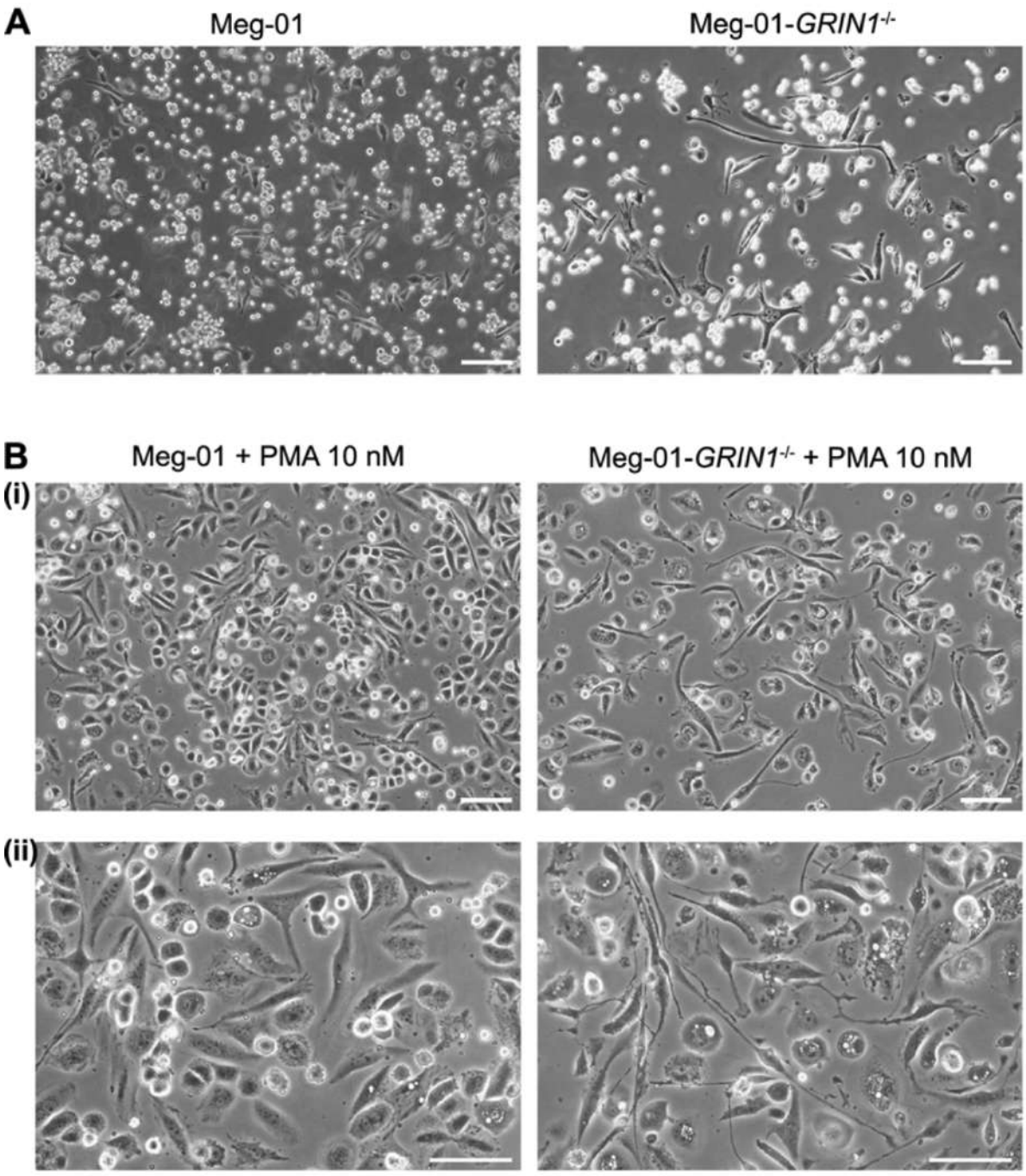

Supplementary Fig. S13. Morphological effects of PMA on Meg-01 and Meg-01-*GRIN1*$^{-/-}$ cells. (**A**) Morphology of Meg-01 and Meg-01-*GRIN1*$^{-/-}$ cells seen at baseline and after 3 days of culture in the presence of 10 nM PMA (**B**). Representative images are shown taken by phase contrast microscopy at lower (20x; **Bi**) and higher (40x; **Bii**) magnifications. PMA

increased numbers of large, adherent cells for both Meg-01 and Meg-01-*GRIN1*$^{-/-}$ cells. Prominent vacuolation persisted in Meg-01-*GRIN1*$^{-/-}$ cells. Scale bars, 100 μm

Supplementary Fig. S14

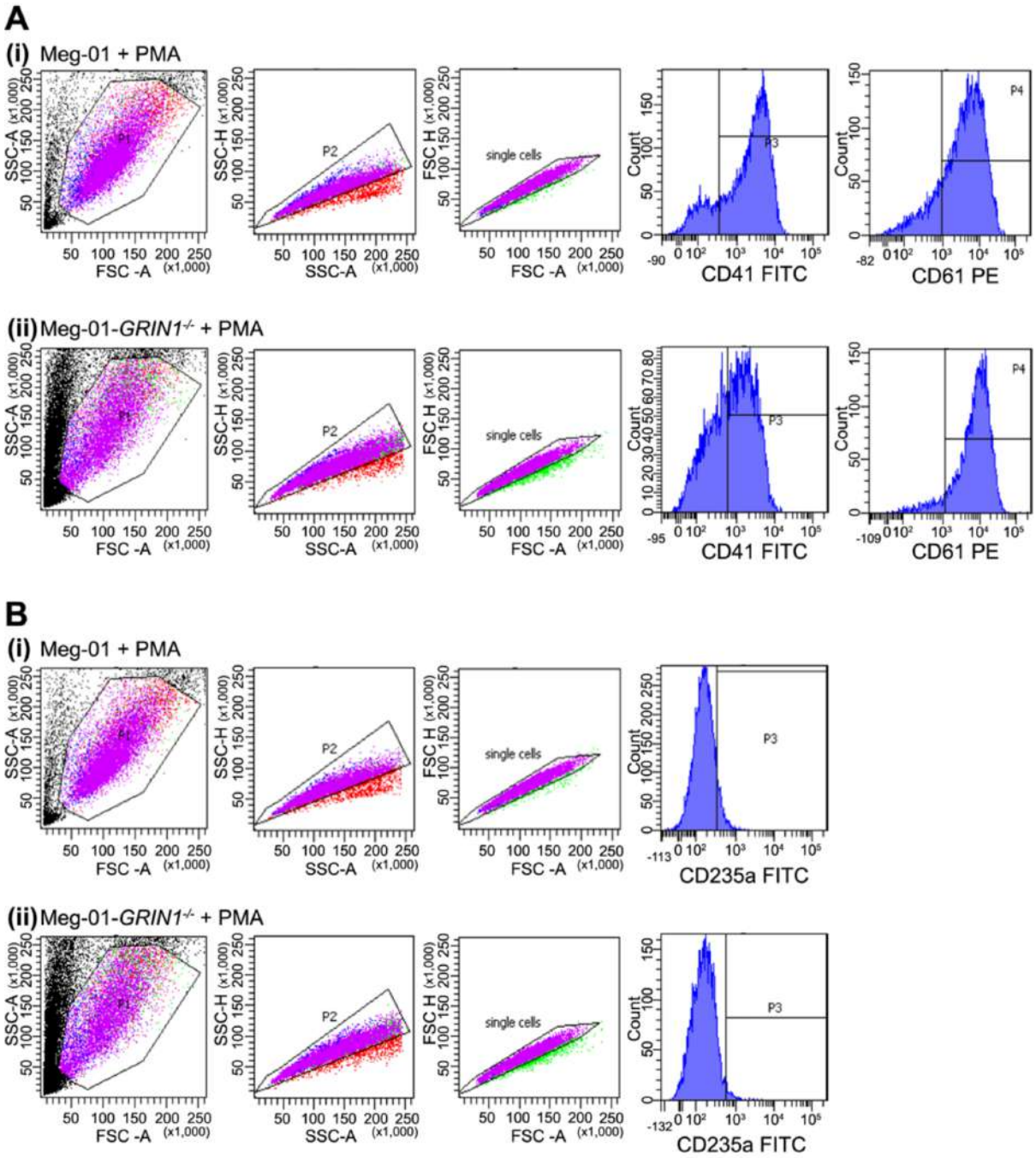

Supplementary Fig. S14. Flow cytometry gates for CD41, CD61 (**A**) and CD235a (**B**) on PMA treated Meg-01 and Meg-01-*GRIN1*$^{-/-}$ cells (**i** and **ii**, respectively). Cells were gated based on forward and side scatter properties (FSC-A vs SSC-A). Cell doublets were excluded by gating on height and area for side scatter (SSC-H vs SSC-A) and forward scatter (FSC-H

vs FSC-A), respectively. Histogram examples of CD41, CD61 and CD235a expression (CD41-FITC, CD61-PE, CD235a-FITC) are shown.

Supplementary Table S1. Quantitative RT-PCR primers used in this study.

Gene name **NCBI number**	**Primer sequence 5' to 3'** **or a catalogue number**	**Reference**
ER stress genes		
CHOP/DDIT3 NM_001195057	F: GGAGCATCAGTCCCCCACTT R: TGTGGGATTGAGGGTCACATC	[1] van Galen et al. 2014
GRP78/HSPA5 NM_005347	F: TGACATTGAAGACTTCAAAGCT R: CTGCTGTATCCTCTTCACCAGT	
ATF4 NM_001675	F: GCTAAGGCGGGCTCCTCCGA R: ACCCAACAGGGCATCCAAGTCG	
GADD34/PPP1R15A NM_014330	F: CCCAGAAACCCCTACTCATGATC R: GCCCAGACAGCCAGGAAAT	
XBP1total NM_005080	F: GGCATCCTGGCTTGCCTCCA R: GCCCCCTCAGCAGGTGTTCC	
XBP1spliced NM_001079539	F: CGCTTGGGGATGGATGCCCTG R: CCTGCACCTGCTGCGGACT	
NMDAR genes		
GRIN1 NM_007327	**F**: TCCCTGTCCATCCTCAAGTC **R**: CTGATACCGAACCCACGTCT	[2] Kalev-Zylinska et al. 2014
GRIN2A NM_000833	**F**: TTGCTTCAGTTTGTGGGTGA **R**: GTTGTGGCAGATCCCAGTG	
GRIN2B NM_000834	**F**: AGCAATGGGACTGTCTCACC **R**: AACATCATCACCCATACGTCAG	
GRIN2C NM_000835	**F**: AGCCCTGGTGGGTACCTG **R**: TCATGTATAGGACGCCATGC	
GRIN2D NM_000836	**F**: GGCTCAGTGACCGCAAGT **R**: GCACGGTCCCAAACTTCA	
GRIN3A NM_133445	**F**: TGCTGACTGCAAACTTCTCAC **R**: AGGCCAATGCCGTATCCT	
GRIN3B NM_138690	**F**: CATGGTCGGGGACAAGAC **R**: GGAAGCTCTTCTTGATGTACGC	
Microarray validation genes		
ERG NM_001136155	Hs.PT.58.1201218	catalogue # (IDT)
FLI1 NM_001167681	Hs.PT.58.26907335	
SCIN NM_001112706	Hs.PT.58.40579814	
RUNX1 NM_001001890	Hs.PT.58.24461868	
HEY1 NM_012258	Hs.PT.58.4299267	
KFL3 NM_016531	Hs.PT.58.14796396	
GATAD1 NM_021167	Hs.PT.58.4070397	

CREBRF NM_001168393	Hs.PT.58.21376072	
ID1 NM_002165	Hs.PT.58.18791272.g	
ID3 NM_002167	Hs.PT.58.28216021.g	
JUN NM_002228	Hs.PT.58.25094714.g	
NFATC1 NM_006162	Hs.PT.58.41101672	
CALB1 NM_004929	Hs.PT.56a.20522981	
CALN1 NM_001017440	Hs.PT.58.19477773	
ATP2A3 NM_005173	Hs.PT.56a.40402270.g	
ATP2B4 NM_001001396	Hs.PT.56a.21466639.g	
SLC24A3 NM_020689	Hs.PT.58.2913018	
TRPC6 NM_004621	Hs.PT.58.23046270	
Reference genes		
HPRT1 NM_000194	F: CCAGTCAACAGGGGACATAAA R: CACAATCAAGACATTCTTTCCAGT	[3] Singleton et al. 2015
LMNA NM_170707	F: TGAGGCCAAGAAGCAACTTCA R: CTCATGACGGCGCTTGGT	[4] Lasham et al. 2010
GAPDH NM_002046	Hs.PT.39a.22214836	

IDT, Integrated DNA Technologies.

References:

1 van Galen P, Kreso A, Mbong N, et al. The unfolded protein response governs integrity of the haematopoietic stem-cell pool during stress. Nature 2014;510:268-272.

2 Kalev-Zylinska ML, Green TN, Morel-Kopp MC, et al. N-methyl-D-aspartate receptors amplify activation and aggregation of human platelets. Thromb Res 2014;133:837-847.

3 Singleton DC, Rouhi P, Zois CE, et al. Hypoxic regulation of RIOK3 is a major mechanism for cancer cell invasion and metastasis. Oncogene 2015;34:4713-4722.

4 Lasham A, Herbert M, Coppieters 't Wallant N, et al. A rapid and sensitive method to detect siRNA-mediated mRNA cleavage in vivo using 5' RACE and a molecular beacon probe. Nucleic Acids Res 2010;38:e19.

Supplementary Table S2. Expression of the calcium toolkit genes in Meg-01-*GRIN1*$^{-/-}$ cells compared with unmodified Meg-01 cells identified by Clariom S microarrays.

Protein name	Gene name	Meg-01-*GRIN1*$^{-/-}$ cells	Meg-01 cells	FC	*P*-value	FDR
Voltage Operated Calcium Channels						
Cav1.1	*CACNA1S*	4.12	4.05	1.07	0.7378	0.8909
Cav1.3	*CACNA1D*	4.65	4.31	1.27	0.8174	0.9281
Cav1.4	*CACNA1F*	3.75	3.72	1.02	0.4797	0.7335
Cav2.1	*CACNA1A*	5.96	7.13	-2.26	0.0007	0.0107
Cav2.2	*CACNA1B*	4.63	4.38	1.18	0.1284	0.3722
Cav2.3	*CACNA1E*	4.41	4.55	-1.1	0.5974	0.8111
Cav3.1	*CACNA1G*	4.47	4.47	1	0.9249	0.9716
Cav3.2	*CACNA1H*	5.17	5.62	-1.37	0.0146	0.0947
Cav3.3	*CACNA1I*	5.16	5.33	-1.12	0.3617	0.6441
Store-Operated Calcium Entry Players						
Orai1	*ORAI1*	6.86	7.29	-1.35	0.0186	0.1116
Orai2	*ORAI2*	6.56	6.55	1	0.492	0.7430
Orai3	*ORAI3*	6.56	6.44	1.08	0.5031	0.7502
STIM1	*STIM1*	8.48	8.69	-1.15	0.1511	0.4072
STIM2	*STIM2*	5.06	4.97	1.06	0.2303	0.5140
CRACR2A	*EFCAB4B*	7.12	7.2	-1.06	0.4128	0.6845
MS4A12	*MS4A12*	4.11	3.86	1.18	0.1056	0.3316
TRP Channels						
TRPA1	*TRPA1*	2.18	2.11	1.05	0.7296	0.8865
TRPC1	*TRPC1*	4.14	3.84	1.24	0.3181	0.6061
TRPC3	*TRPC3*	3.54	4.1	-1.48	0.2155	0.4963
TRPC4	*TRPC4*	3.38	3.47	-1.06	0.7874	0.9142
TRPC5	*TRPC5*	3.55	3.54	1.01	0.8015	0.9205
TRPC6	*TRPC6*	3.84	6.56	-6.61	9.69E-10	6.31E-07
TRPC7	*TRPC7*	4.68	4.6	1.06	0.5454	0.7799
TRPV1	*TRPV1*	5.91	6.21	-1.23	0.4084	0.6813
TRPV2	*TRPV2*	7.36	7.28	1.06	0.7274	0.8856
TRPV3	*TRPV3*	4.46	4.24	1.17	0.1792	0.4481
TRPV4	*TRPV4*	3.72	3.54	1.13	0.4943	0.7443
TRPV5	*TRPV5*	4.25	4.19	1.04	0.8469	0.9409
TRPV6	*TRPV6*	4.92	5.14	-1.16	0.0694	0.2600
TRPM1	*TRPM1*	4.38	4.64	-1.2	0.1596	0.4192
TRPM2	*TRPM2*	6.28	6.38	-1.07	0.7168	0.8803
TRPM3	*TRPM3*	4.1	4.26	-1.11	0.2117	0.4922
TRPM4	*TRPM4*	7.25	7.57	-1.25	0.0181	0.1096
TRPM5	*TRPM5*	5.08	5.09	-1.01	0.865	0.9478
TRPM6	*TRPM6*	3.65	3.97	-1.25	0.6404	0.8375
TRPM7	*TRPM7*	7.29	7.28	1	0.2946	0.585
TRPM8	*TRPM8*	4.98	4.58	1.32	0.441	0.705
TRPML1	*MCOLN1*	8.92	9	-1.05	0.9347	0.9755
TRPML2	*MCOLN2*	4.47	5.39	-1.89	0.0196	0.1159

TRPML3	*MCOLN3*	3.68	2.27	2.64	0.0003	0.0056
TRPP1	*PKD2*	5.73	5.94	-1.16	0.0485	0.2087
TRPP2	*PKD2L1*	3.22	3.39	-1.13	0.3476	0.6321
TRPP3	*PKD2L2*	2.54	2.37	1.12	0.3056	0.596
Calcium Release Channels						
IP3R1	*ITPR1*	7.22	7.66	-1.36	0.0088	0.0672
IP3R2	*ITPR2*	5.63	5.65	-1.02	0.741	0.8931
IP3R3	*ITPR3*	4.76	4.59	1.13	0.856	0.9441
RYR1	*RYR1*	5.98	5.99	-1.01	0.9208	0.9701
RYR2	*RYR2*	4.59	4.65	-1.04	0.913	0.9669
RYR3	*RYR3*	2.81	3.55	-1.68	0.0061	0.0514
Calcium Pumps						
PMCA1	*ATP2B1*	7.29	7.18	1.08	0.5669	0.7935
PMCA2	*ATP2B2*	6.44	6.69	-1.19	0.3939	0.6711
PMCA3	*ATP2B3*	6.82	6.92	-1.07	0.3486	0.6327
PMCA4	*ATP2B4*	6.88	7.72	-1.78	0.0004	0.0066
SERCA1	*ATP2A1*	5.85	5.8	1.04	0.4659	0.7237
SERCA2	*ATP2A2*	10.67	10.75	-1.05	0.3756	0.6558
SERCA3	*ATP2A3*	8.69	9.69	-1.99	1.04E-07	1.71E-05
SPCA1	*ATP2C1*	9.8	9.7	1.07	0.15	0.4056
SPCA2	*ATP2C2*	5.78	5.76	1.02	0.3982	0.6742
Sodium Calcium Exchangers						
NCX1	*SLC8A1*	2.67	2.91	-1.19	0.0298	0.153
NCX2	*SLC8A2*	5	5.18	-1.13	0.7555	0.9002
NCX3	*SLC8A3*	4.84	5.23	-1.3	0.0117	0.0814
Sodium Calcium Potassium Exchangers						
NCKX1	*SLC24A1*	4.77	5.03	-1.2	0.0340	0.1667
NCKX2	*SLC24A2*	3.2	3.51	-1.23	0.0930	0.3066
NCKX3	*SLC24A3*	5.56	7.13	-2.97	1.42E-08	4.29E-06
NCKX4	*SLC24A4*	3.46	3.59	-1.1	0.4065	0.6797
NCKX5	*SLC24A5*	3.58	3.43	1.11	0.5992	0.8122
NCKX6	*SLC8B1*	8.82	8.58	1.18	0.0377	0.1779
Mitochondrial Calcium Transport Proteins						
MCU	*MCU*	7.75	7.81	-1.04	0.6003	0.8127
MICU1	*MICU1*	8.41	8.04	1.3	0.02	0.1174
MICU2	*EFHA1*	6.61	6.76	-1.11	0.2273	0.5103
MICU3	*EFHA2*	2.78	2.64	1.11	0.4205	0.691
MCUR1	*CCDC90A*	9.32	9.56	-1.19	0.0317	0.159
EMRE	*C22orf32/SMDT1*	8.45	8.4	1.03	0.3579	0.6411
MCUb	*CCDC109B*	4.68	4.21	1.39	0.0803	0.2818
VDAC1	*VDAC1*	10.37	10.37	-1	0.9518	0.982
VDAC2	*VDAC2*	11.39	11.26	1.1	0.2236	0.5055
VDAC3	*VDAC3*	10.32	10.31	1.01	0.7167	0.8802
Other Regulators						
Bcl-2	*BCL2*	6.96	7.37	-1.33	0.0041	0.0391
Calsequestrin 1	*CASQ1*	5.7	5.73	-1.02	0.6593	0.8488
Calsequestrin 2	*CASQ2*	2.56	2.7	-1.1	0.0827	0.2862

PICALM	*PICALM*	11.38	11.51	-1.1	0.1068	0.3336
Calreticulin	*CALR*	12.64	12.68	-1.03	0.4100	0.6823
Calnexin	*CANX*	11.51	11.39	1.09	0.2612	0.5488
Phospholamban	*PLN*	2.74	2.9	-1.12	0.7317	0.8879
Calbindin 1	*CALB1*	9.34	7.45	3.73	5.26E-08	1.05E-05
Calbindin 2	*CALB2*	4.46	4.64	-1.14	0.4745	0.7310
Calneuron 1	*CALN1*	2.81	5.87	-8.38	1.24E-10	1.84E-07
Scinderin	*SCIN*	5.3	3.02	4.85	1.64E-07	2.41E-05

Differentially expressed genes are highlighted in yellow (FC $\geq$ 1.5 and FDR $\leq$ 0.05).

Abbreviations: FC, fold change; FDR, false discovery rate.

Supplementary Table S3. Differential expression of molecules defining or associated with erythroid or megakaryocytic differentiation in Meg-01-*GRIN1*$^{-/-}$ cells compared with unmodified Meg-01 cells, identified by Clariom S microarrays.

Gene	Gene product	Fold change	*P*-value	FDR
Erythroid defining/associated molecules				
HBE1	Hemoglobin subunit epsilon 1	5.04	4.40E-11	8.58E-08
ALAS2	5-aminolevulinate synthase 2, erythroid	4.56	2.78E-09	1.24E-06
HBZ	Hemoglobin subunit zeta	2.92	3.58E-06	2.00E-04
HEMGN	Hemogen	2.71	6.45E-08	1.19E-05
UROD	Uroporphyrinogen decarboxylase	2.23	7.41E-08	1.31E-05
SLC4A1	Solute carrier family 4 (anion exchanger), member 1 (Band 3)	2.17	4.04E-06	3.00E-04
ERMAP	Erythroblast membrane associated protein	2.11	2.43E-06	2.00E-04
EPB41L4B	Erythrocyte membrane protein band 4.1 like 4B	2.10	5.33E-05	1.70E-03
RHCE	Rh blood group CcEe antigens	2.02	5.44E-05	1.70E-03
EPB42	Erythrocyte membrane protein band 4.2	1.94	1.54E-05	7.00E-04
SPTA1	Spectrin alpha, erythrocytic 1	1.90	2.50E-03	2.75E-02
TFRC	Transferrin receptor	1.86	2.25E-06	2.00E-04
EPB42	Erythrocyte membrane protein band 4.2	1.85	2.86E-06	2.00E-04
SPTB	Spectrin beta, erythrocytic	1.80	3.66E-08	8.00E-06
HMBS	Hydroxymethylbilane synthase	1.56	2.00E-04	4.60E-03
RHD	Rh blood group D antigen	1.53	1.30E-03	1.75E-02
KEL	Kell metallo-endopeptidase	1.53	7.74E-05	2.20E-03
EPOR	Erythropoietin receptor	1.51	1.00E-03	1.40E-02

Megakaryocyte defining/associated molecules				
VWA5A	Von Willebrand factor A domain containing 5A	8.8	5.19E-10	4.08E-07
CD9	CD9	2.46	2.38E-07	3.15E-05
PDGFD	Platelet derived growth factor D	1.83	8.00E-04	1.25E-02
VWA8	Von Willebrand factor A domain containing 8	1.56	3.00E-04	5.60E-03
GP6	Glycoprotein VI	-1.56	1.77E-05	7.00E-04
GP9	Glycoprotein IX	-1.56	1.40E-03	1.76E-02
CD47	CD47 molecule	-1.57	4.03E-05	1.30E-03
ITGA2B	Integrin alpha 2b (CD41)	-1.63	3.10E-06	2.00E-04
SPARC	Secreted protein, acidic, cysteine-rich	-1.94	3.26E-06	0.0002
GP1BA	Glycoprotein Ib (platelet), alpha polypeptide (CD42b)	-2.01	2.35E-06	2.00E-04
TMEM71	Transmembrane protein 71	-2.23	3.00E-04	5.30E-03
VWDE	Von Willebrand factor D and EGF domains	-2.57	3.59E-07	4.29E-05
MAP1B	Microtubule associated protein 1B	-10.01	8.24E-09	3.05E-06

FDR, False Discovery Rate.

Supplementary Microarray Excel Data File S1. Full list of gene expression data in Meg-01-*GRIN1*$^{-/-}$ cells and unmodified Meg-01 cells obtained from Clariom S microarrays.

See a separate file.